Functional resting state networks characterization through global network measurements for patients with disorders of consciousness
Caracterización de redes funcionales en estado de descanso a través de medidas globales de redes para pacientes con desórdenes de conciencia

Darwin E. Martínez*†, Johann H. Martínez‡§, Jorge Rudas†, Athena Demertzi¶, Lizette Heine¶, Luaba Tshibanda¶, Andrea Soddu‖, Steven Laureys¶, and Francisco Gómez*
*Computer Science Department
Universidad Central, Bogotá, Colombia
Email: dmartinezr6@ucentral.edu.co
†Universidad Nacional de Colombia, Bogotá, Colombia
‡Universidad Politécnica de Madrid, Madrid, Spain
§Universidad del Rosario, Bogotá, Colombia
¶Cyclotron Research Center, University of Liège, Liège, Belgium
‖Physics and Astronomy Department, Western University, London, Canada

***Abstract*—Disorders of consciousness (DOC) is a consequence of severe brain injuries. DOC diagnosis is quite challenging because it may require patient collaboration. Investigations of brain activity in resting conditions propose that healthy brain is organized into large-scale resting state networks (RSNs) of sensory/cognitive relevance. The complete set of RSN together with their corresponding interaction induce a functional network of brain connectivity (FNC). Recently, the connectivity pattern between pairs of RSNs have been explored as biomarker of loss of consciousness. The role of this FNC in the DOC conditions remains poorly understood. In this work, we propose to use a network analysis method to explore complex properties of the functional brain network induced by the connectivity among RSNs. In particular, we aim to characterize the communication quality among network nodes, which have been suggested to be linked to altered states of consciousness. The proposed approach was evaluated on a population of 27 healthy controls and 49 subjects with DOC conditions. fMRI data was obtained and processed for each subject to built a FNC at individual level. The communication quality among network nodes was quantified by using global efficiency, average characteristic path, diameter, radius, average strength and average clustering coefficient. Our results suggests that the information efficiency transfer at the global level decrease with the level the severity of the loss of consciousness condition. These results highlight the importance of graph based features to characterize brain complexity, and in particular, complex phenomena as consciousness emergence. In addition, our results can be potentially used in the development of novel methods to support diagnosis of patients with DOC conditions.**

***Keywords*—Disorders of Consciousness; Resting state networks; Complex graph theory; Global efficiency.**

***Abstract*—Los desórdenes de conciencia son consecuencia de accidentes cerebrales severos. El diagnóstico de estas condiciones constituye un reto, dado que las evaluaciones diagnósticas usuales pueden requerir de la colaboración del paciente. Investigaciones de la actividad cerebral de sujetos sanos durante estado de descanso se organiza en redes de descanso de relevancia sensorial/cognitiva. A su vez, las interacciones entre estas redes inducen una red cerebral de conectividad funcional. Recientemente, los patrones de conectividad entre pares de redes de descanso han sido explorados como biomarcadores de estados de conciencia alterada. Sin embargo, el papel de la conectividad funcional entre redes de descanso en los desórdenes de conciencia es poco conocido. En este trabajo se propone un análisis basado en teoría de grafos para la caracterización de la red de conectividad funcional. En particular, se busca describir la calidad de la comunicación entre los nodos de esta red en estados alterados de conciencia. Esta caracterización se realizó en una población de 27 sujetos sanos y 49 sujetos con diagnóstico de DOC. Para esto, datos de fMRI fueron obtenidos y procesados para cada sujeto con el fin de construir su red de conectividad funcional. La calidad de la comunicacin entre nodos de la red se cuantificó utilizando medidas globales de redes, incluyendo: eficiencia global, ruta característica promedio, diámetro, radio, promedio de potencia y promedio del coeficiente de agrupamiento. Los resultados indican que la eficiencia en la transferencia de información se reduce con el nivel de severidad de la condición de perdida de conciencia. Estos resultados resaltan la importancia del uso de caracterizaciones basada en grafos para el entendimiento de los mecanismos de conciencia. Adicionalmente, estos hallazgos pueden utilizarse para el desarrollo de nuevos métodos que soporten el diagnóstico de pacientes con condiciones de DOC.**

978-1-4673-9464-2/15/$31.00 ©2015 IEEE

I. Introduction

Disorders of consciousness (DOC) encompass a set of particular conditions after a coma state. These conditions can result from traumatic and non-traumatic brain injuries. It includes minimally conscious state (MCS), vegetative state/unresponsive wakefulness state (VS/UWS) and brain death [1], [2]. Patients with DOC are commonly severely affected in their brain structure [3], [4] and function [5]. Diagnosis of these conditions is typically performed by using a variety of neurophysiological assessments, such as, the coma recovery scale [6], [7] or the Rancho los amigos sacle [8]. The diagnosis of this conditions is a very challenging task because it may requires the patient collaboration [9]. Therefore, alternative approaches that overcome this limitation should be employed to improve diagnosis and understand of these pathological brain conditions. These approaches may include different brain function and structure measurements [10] including electroencephalography (EEG) [11], and a variety of brain imaging techniques as functional magnetic resonance imaging (fMRI) [12] and diffusion weighted magnetic resonance imaging (diffusion MRI) [13], among others. Neuroimaging allows to observe in-vivo structure and function of the brain. In particular, functional magnetic resonance imaging characterizes the dynamical brain behavior [14]–[16].

During the last two decades, brain activity registered at rest have been explored as an objective alternative to construct bio-markers of different pathological brain conditions [17]. Resting state protocols were proposed to get information of the brain activity while it is at rest, i.e., while the brain is not exposed to any stimuli [18], [19]. For DOC patients resting state protocols has been explored on distinct brain function modalities including, EEG and fMRI [20]–[22]. Research in brain activity in resting conditions suggests that healthy brain is organized into large-scale resting state networks (RSNs) of sensory/cognitive relevance [23], [24]. Different strategies have been employed to characterize RSNs. One of the most common approaches is based on the analysis of independent components (ICA) [25], [26] which looks for functional connectivity of spatially segregated brain areas. Other approaches include seed based methods [27], principal component analysis (PCA) [28] and clustering techniques [29]. At least ten of these resting state networks (RSNs) have been consistently identified in healthy control subjects [30]. Including: auditory, cerebellum, default mode network, executive control left, executive control right, saliency, sensori-motor, visual lateral, visual media and visual occipital. Understanding of the dynamic and the activation patterns of these resting state networks for healthy controls and patients in pathological conditions is an unsolved research question [31]. Alterations of the connectivity levels in the RSNs have been proposed as bio-markers for the study of a variety of pathological conditions [17] including, Alzheimer [26], [32] and Schizophrenia [15], among others.

Recently, a complementary RSNs analysis strategy that considers the functional relationship among RSNs has been explored in the so called functional network connectivity (FNC). FNC studies are focused in the assessment of the level of interaction during spontaneous activity among different RSNs [33]. This brain dynamic picture is constructed by computing pairwise measurements of connectivity between the RSNs time courses. Typical measurements of interaction include: Pearson's correlation coefficient that aims to capture linear relationships among the time courses [34], Granger causality that characterizes directional connectivity [35], and temporal slicing window that allows to explore temporal changes in the RSN connectivity [36]. Most of these approaches are based on the underlying assumption that RSN brain dynamics follows linear regimes. However, recent evidence suggests that neuronal function of cortical ensembles during resting state may follow non-linear behaviors [37]. Therefore, usual interaction measurements may be limited to capture this phenomenon. An alternative approach to characterize these non-linear conditions is based on the distance correlation that aims to capture relationships with non-linear behavior between different RSNs [38]. In addition, the level of interaction among RSNs has been recently explored as a possible biomarker of loss-of-consciousness [5], [30], [33].

FNC allows to explore and identify functional connections between specific brain regions. It also provides important insights about overall organization of functional communication in the brain network [30], [39]. Early approaches using resting state neuroimaging were focused on functional connectivity variations [12]. Nevertheless, in the last decade, graph theory or complex network analysis has been proposed as powerful approach to get insight into brain organization and function [40]–[42]. Brain can be understood as a network which consist of spatially distributed but functionally linked regions that continuously share information each other [39], and graph theory approaches provides powerful tools to understand how brain pathological conditions can affect graph brain properties [12], [42], [43]. Graph theory measurements has been used to understand function affectations and reconfigurations in pathological brain conditions such as, Alzheimer [26], [32], [44], Schizophrenia [15], [45] and Autism [45], among other conditions. Graph theory has been also applied to study relationships among resting state networks, and their topological structure [46]. Although brain networks alterations were consistently related with some brain affectations, for DOCs conditions graph properties remain poorly understood [31].

In this work, we propose the use of complex graph characterization features computed on the brain network generated by the FNC as a bio-marker for DOC conditions. In particular, we propose to use global network measurements - global efficiency, average characteristic path, diameter, radius, average strength and average clustering coefficient - to depict how brain works in DOC conditions. Particularly to get insight about the communication quality among FNC nodes.

II. Materials and methods

The figure 1 illustrates the proposed characterization. First, functional images at rest were acquired. Following, spatial independent component analysis was computed. Next, a template matching algorithm was used to select the different RSNs. Then, FNC brain graph was calculated. Finally, global network measurements on this network were computed.

A. Participants and data acquisition

Acquisitions from 76 subjects were used for this study: 27 healthy controls (14 women, mean age 47 $\pm$ 16 years), 24 patients in minimal conscious state and 25 with vegetative

state/unresponsive wakefulness syndrome (20 women, mean age 50 $\pm$ 18 years), more details about the patients demography can be found in [19]. Data were acquired in the Hospital University of Liège. For each subject, fMRI resting state data were acquired in a 3T scanner (Siemens medical Solution in Erlangen, Germany). Three hundred fMRI volumes multislice T2-weighted functional images were captured (32 slices; voxel size: $3 \times 3 \times 3$ mm^3; matrix size $64 \times 64 \times 32$; repetition time = 2000 ms; echo time = 30 ms; flip angle = 78°; field of view = 192×192 mm^2) see Figure 1(a). Also, a structural T1 image was acquired for anatomical reference. All patients were clinically examined using the French version of the Coma Recovery Scale Revised (CRS-R) [47], and written informed consent to participate in the study was obtained from all patients or legal surrogates of the patients. The healthy volunteers were instructed to close their eyes, relax without falling a sleep and refrain from any structured thinking (e.g., counting, singing etc.). The same instructions were given to patients but due to their cognitive and physical impairments, we could not fully control for a prolonged eye-closed yet awake scanning session.

B. Preprocessing

Preprocessing of fMRI data was performed using SPM[1] [48]. Preprocessing included: realignment, co-registration of functional onto structural data, segmentation of structural data, normalization into MNI space and spatial smoothing with a Gaussian kernel of $8\ mm$. After, large head motions were corrected using ArtRepair [49].

1) Spatial Independent Component Analysis: The first step for the RSN identification was the fMRI signal decomposition into sources of neuronal/physiological origin, see Figure 1(b). For this task, we used ICA, which aims to decompose the signal into a set of statistically independent components (ICs) of brain activity. Because in the fMRI data the spatial dimension is much greater than temporal one, we used spatial ICA (sICA), which decompose the signal into maximally independent spatial maps [50]. In sICA each spatial map (source fMRI signal) has an associated time course, which corresponds to the common dynamic exhibit by this component. These RSN time courses were subsequently used for all the FNC computations. For the ICA decomposition we used 30 components and the infomax algorithm as implemented in GroupICA [14] toolbox[2].

2) RSNs Identification: After the ICA decomposition, the different RSNs were identified at individual level, see Figure 1(c). The main common approach for this task is the group level identification. In this method, the fMRI data of whole population is concatenated along the temporal dimension. Later, sICA is applied to identify the sources of brain activity at the group level. Following, each RSN is manually identified [34]. Finally, individual time courses are extracted for each RSN by applying a dual regression (back-reconstruction) onto the original subject data [34]. This approach is based on a homogeneity assumption of the fMRI dynamic across the whole population. Nevertheless, in severely affected brains, this condition may be not valid [19]. In order to overcome this limitation, a single subject RSN identification approach was used [19]. This approach is based on a twofold process: template matching and artifactual classification.

Template Matching: We used an alternative approach that aims identifying each RSN directly from the single subject sICA decomposition. In particular, we ran a single subject sICA. Then, the set of ICs that maximize the similarity with a set of RSN templates (figure 1) were selected for clinical specialists [19]. This approach has been proved to be robust in non-homogenous populations, as the herein studied, and it can be used directly for individual assessment of subjects in clinical applications.

Artifactual Classification: After the RSN spatial map identification, a machine learning based labeling method was applied to discriminate between independent components of "neuronal" or "artifactual" origin. We used the approach proposed in [19]. In particular, it was used a binary classification method based on support vector machines (SVM) which were trained on 19 independently assessed healthy subjects. A set of a spatio-temporal feature vector for description each IC was obtained from ICA decomposition (n = 30 components). Each feature vector contains both spatial (i.e., degree of clustering, skewness, kurtosis, spatial entropy) and temporal information (i.e., one-lag autocorrelation, temporal entropy, power of five frequency bands: 0 to 0.008 Hz, 0.008 to 0.02 Hz, 0.02 to 0.05 Hz, 0.05 to 0.1 Hz, and 0.1 to 0.25 Hz) [19].

3) Functional network connectivity: In order to characterize of interactions between the different RSNs we computed the Functional Network Connectivity (FNC) [34] matrix among the previously selected networks, see Figure 1(d). The objective in FNC is to measure the strength of the interactions between the different RSNs. These interactions were computed by measuring the level of dependency between the corresponding RSN time courses [34].

In this work, we used distance correlation (DC) [51] to compute the FNC matrix. Distance correlation aims to measure non-linear dependencies between two random variables X and Y with finite moments in arbitrary dimension [51].

DC can be defined based on an observed random sample $(X, Y) = \{(X_k, Y_k)|k = 1, 2, \ldots, n\}$ of the joint distribution of random vectors X in $\mathbb{R}^p$ and Y in $\mathbb{R}^q$. Using these samples a transformed distance matrix A can be defined as follows:

$$a_{kl} = \|X_k - X_l\| \qquad \bar{a}_{k\cdot} = \frac{1}{n}\sum_{l=1}^{n} a_{kl} \qquad \bar{a}_{\cdot l} = \frac{1}{n}\sum_{k=1}^{n} a_{kl},$$

$$\bar{a}_{\cdot\cdot} = \frac{1}{n^2}\sum_{k,l=1}^{n} a_{kl} \qquad A_{kl} = a_{kl} - \bar{a}_{k\cdot} - \bar{a}_{\cdot l} + \bar{a}_{\cdot\cdot}$$

$k, l = 1, 2, \ldots, n$. Similarly, a matrix B can be defined to characterize distances between samples for Y. Following, the empirical distance is defined by $V_n^2(X, Y) = \frac{1}{n^2}\sum_{k,l=1}^{n} A_{kl}B_{kl}$. Finally, the empirical DC corresponds to the square root of

$$R_n(X, Y) = \begin{cases} \frac{V_n^2(X,Y)}{\sqrt{V_n^2(X)V_n^2(Y)}} & V_n^2(X)V_n^2(Y) > 0 \\ 0 & V_n^2(X)V_n^2(Y) = 0 \end{cases}$$

[1] http:www.fil.ion.ucl.ac.uk/spm

[2] http://icatb.sourceforge.net/

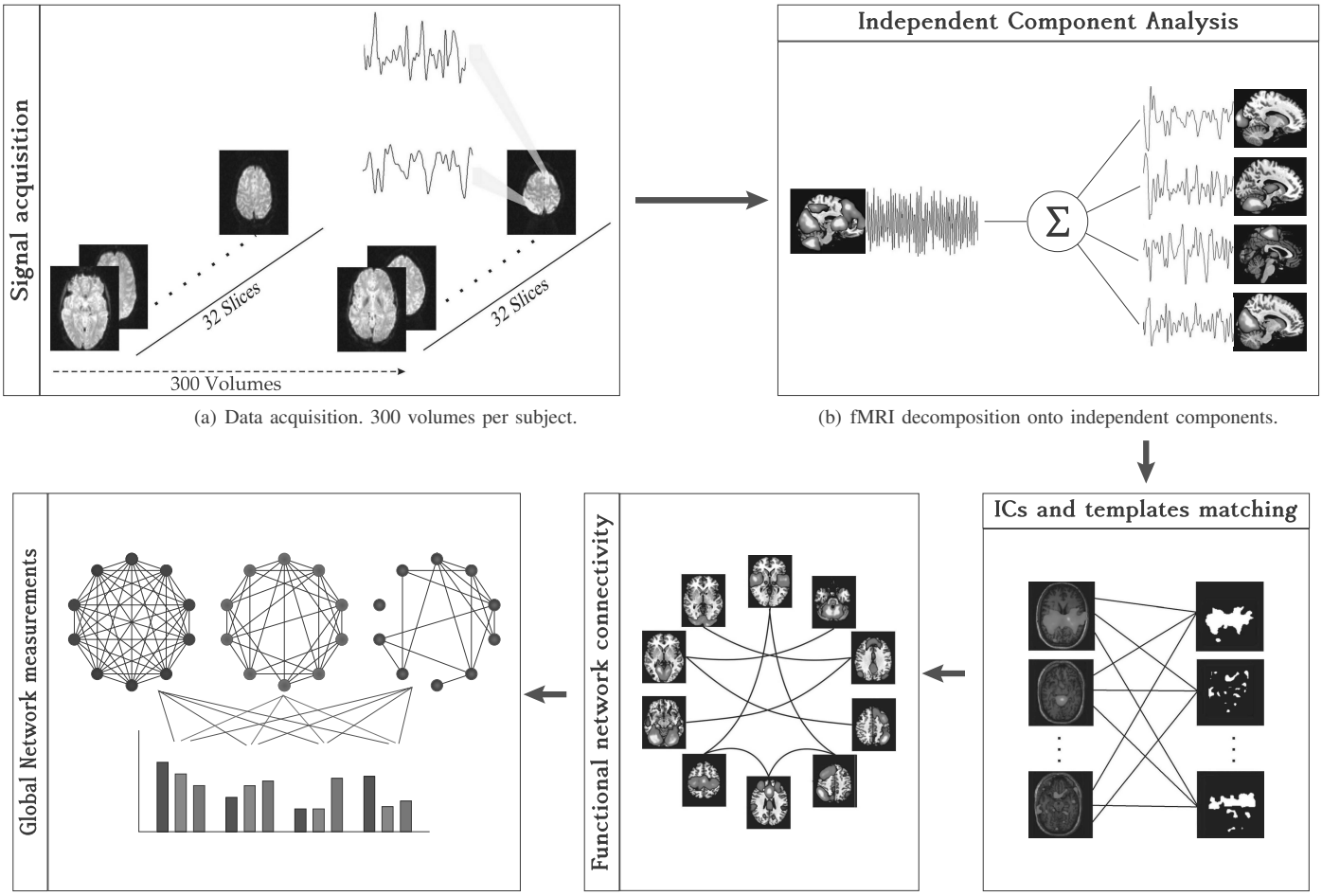

(a) Data acquisition. 300 volumes per subject.

(b) fMRI decomposition onto independent components.

(c) RSN identification: template matching and artifactual classification.

(d) Functional network connectivity computation through distance correlation.

(e) Illustration of global network measurements over FNC (Healthy-blue, MCS-green, VS/UWS-red)

Fig. 1. Main process workflow: data acquisition, preprocessing (Spatial independent component analysis, matching between Independent components and templates, and Functional Network Connectivity) and global network measurements.

where $V_n^2(X) = V_n^2(X,X)$. Note that A and B can be computed independently of p and q, and both contain information about between sample elements distances in X and Y. $V_n^2(X,Y)$ is a measure of the distance between the probability distribution of the joint distribution and the product of the marginal distributions, i.e., $V_n^2(X,Y)$ quantifies $\|f_{X,Y} - f_X f_Y\|$, with f_X and f_Y the characteristic function of X and Y respectively and $f_{X,Y}$ the joint characteristic function [51]. In contrast to PC, $V_n^2(X,Y)$ vanish if and only if X and Y are independent variables [51]. The DC corresponds to a normalized version of $V_n^2(X,Y)$, which takes values between 0 and 1, with zero corresponding to statistical independence between X and Y, and 1 total dependency.

Lagged Distance correlation: For the FNC computations we assumed that two RSN time series X and Y provide the n observations of the joint distribution characteristic of the RSN temporal dynamics. Prior to the DC computations, the RSN time courses were filtered thought a bandpass Butterworth filter with cut-off frequencies set at $0.05\ Hz$ and $0.1\ Hz$. This frequency range was previously used in other studies [19]. Similar to Jafry et al [34], we used a maximum lagged approach. For this, we used the lagged DC (LDC) defined by Rudas et al. [38] as:

$$R_n^{\Delta}(X,Y) = R_n(X,Y^{\Delta})$$

where Y^{Δ} is the time course circularly shifted Δ temporal units. We varied Δ between $+6s$ and $-6s$ in TR units ($2\ s$) [34]. The maximal DC value for the 7 shifts was defined as the interaction measure between the two RSN time courses. This maximal lagged DC was assessed between all pairwise valid combinations (both RSNs labeled as "neuronal") where the number of combinations of 10 RSNs, taken 2 at a time results in $10!/(2!(10-2)!) = 45$ possible combinations [38].

C. Global network properties and measurements

Once the underlying FNC network was constructed a set of global network properties were computed for each individual subject functional network. In this work, we propose to use global efficiency, average characteristic path, diameter, radius, avereage strength and average clustering coefficient [43], [52] to characterize the global network properties to get insight of the expected brain global changes commonly expected in patients with DOC conditions, see Figure 1(e).

For this, first consider $\mathcal{G} = (\mathscr{N}, \mathscr{L})$ a weighted network which consist of two sets, a set of nodes $\mathscr{N}$ and a set of links

$\mathscr{L}$, such that $\mathscr{N} \neq \emptyset$ and $\mathscr{L}$ is a set of unordered pairs of elements of $\mathscr{N}$. Also, n is the number of nodes and l is the number of links. (i, j) denotes a link between nodes i and j; i.e., $i,\ j \in \mathscr{N}$ and $(i, j) \in \mathscr{L}$. a_{ij} is the connection status between i and j: $a_{ij} = 1$ when link (i, j) exists, $a_{ij} = 0$ otherwise. Links (i, j) are associated with connection weights w_{ij}. Following Rubinov et al. [43], we normalize the weights such that $0 \leq w_{ij} \leq 1$ for all i and j. l^w is the sum of all weights in the network, computed as $l^w = \sum_{i,j \in \mathscr{N}} w_{ij}$.

1) Average characteristic path: The average characteristic path is the average shortest path length between all pairs of nodes in the network. It is the most commonly used measure of functional integration [53]. The shortest weighted path length between i and j is defined as $d_{ij}^w = \sum_{a_{uv} \in g_{i \leftrightarrow j}^w} f(w_{uv})$, where f is a map from weight to length and $g_{i \leftrightarrow j}^w$ is the shortest weighted path between i and j [43]. Then, weighted characteristic path length is defined in [54] as:

$$L^w = \frac{1}{n} \sum_{i \in \mathscr{N}} \frac{\sum_{j \in \mathscr{N} j \neq i} d_{ij}^w}{n-1}$$

2) Global efficiency: Global efficiency is defined in [55] as:

$$E^w = \frac{1}{n} \sum_{i \in \mathscr{N}} \frac{\sum_{j \in \mathscr{N} j \neq i} \left(d_{ij}^w\right)^{-1}}{n-1}$$

Path length is the minimum number of edges that must be traversed to go from one node to another. Random and complex networks have short mean path lengths (high global efficiency of parallel information transfer) whereas regular lattices have long mean path lengths. Efficiency is inversely related to path length but is numerically easier to use to estimate topological distances between elements of disconnected graphs [53].

3) Diameter: The diameter is the maximum eccentricity. The eccentricity of a vertex j is the maximum of its finite distances to all other vertices, i.e. $ecc(j) = \max(d_{ij})$ [40]. Then, the diameter of is the maximum eccentricity, $diameter(G) = \max(ecc(j))$ [40].

4) Radius: The radius is the minimum eccentricity of all its vertices in a graph, $radius(G) = \min(ecc(j))$ [40].

In addition to these global measurements, average strength and average clustering coefficient were computed for each subject of the mentioned populations.

5) Average strength: the strength of each node is computed, and the strength of all nodes are averaged for each subject network. The strength of a node i is defined in [43] as: $k_i^w = \sum_{j \in \mathscr{N}} w_{ij}$. Then, the average strength of a network $\mathcal{G} = (\mathscr{N}, \mathscr{L})$ is:

$$\bar{k}^w = \frac{1}{n} \sum_{i \in \mathscr{N}} k_i^w$$

6) Average clustering: the clustering coefficient of each node is computed; then, the clustering coefficient of all nodes in the network are averaged for each subject. The clustering coefficient is a measure of segregation, and the clustering coefficient of the network is defined in [54] as:

$$C = \frac{1}{n} \sum_{i \in \mathscr{N}} C_i = \frac{1}{n} \sum_{i \in \mathscr{N}} \frac{2t_i}{k_i(k_i - 1)}$$

where C_i is the clustering coefficient of a node i ($C_i = 0$ for $k_i < 2$)

All network measurements were computed using the Brain Connectivity Toolbox[3] for matlab.

D. Statistical group analysis

To assess the discrimination power of the herein proposed global network measurements a two sample t-test [56] was computed. For this evaluation we grouped the population to analyze the changes in network properties induced by the pathology. For the statistical analysis the following comparisons were performed: healthy controls versus DoC patients (VS/UWS and MCS), healthy controls versus MCS patients, healthy controls versus VS/UWS patients and MCS patients versus VS/UWS patients.

III. Results

The figure 2 shows the results of computing the average characteristic path for each population. As observed, the characteristic path of the healthy controls was more concentrated around the mean than the one for MCS and VS/UWS patients. The dispersions for healthy controls and MCS patients were similar while this value was higher for VS/UWS patients. This suggests that some networks of patients in this condition may have one or more disconnected groups of nodes. The mean values of the average characteristic path evidenced an increasing tendency from healthy controls to MCS and VS/UWS patients. This may suggests that to reach some point of the network from other point the number of links to traverse was lower in healthy controls than in DOC diagnosed patients.

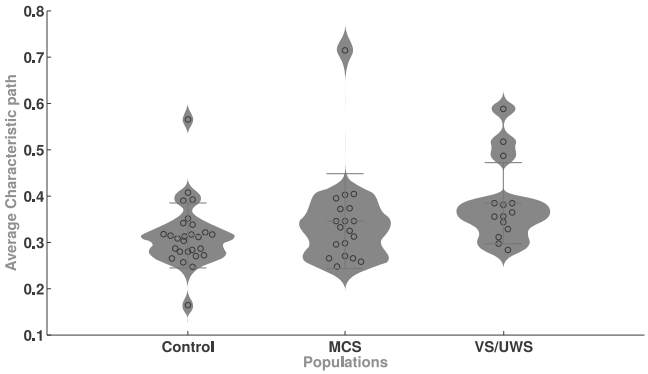

Fig. 2. Distribution of the average characteristic path for healthy control, Minimally conscious state (MCS) and vegetative state/unresponsive wakefulness state (VS/UWS) patients. Points corresponds to different subjects and red bars indicate mean and standard deviation.

Figure 3 shows the global efficiency scores on each network grouped by population. The global efficiency values of healthy control population were higher and more concentrated around the mean than for MCS and VS/UWS patients. The mean values evidenced a decreasing tendency from healthy subjects to MCS and then to VS/UWS patients.

[3]https://sites.google.com/site/bctnet/

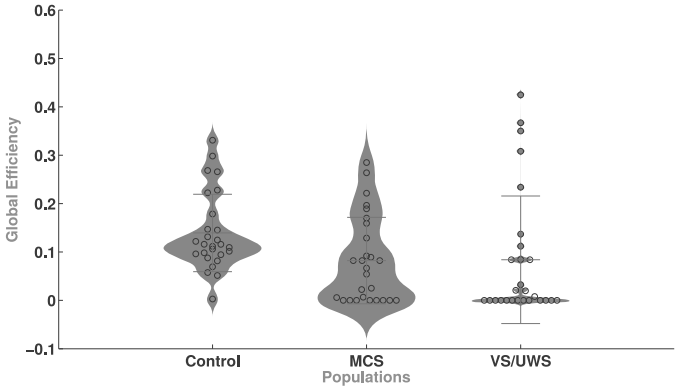

Fig. 3. Distribution of the global efficiency for healthy control, MCS and VS/UWS patients.

The figures 4 and 5 show the results for the diameter and radius, respectively. In both cases, the measurements for healthy subjects were more concentrated around the mean compared to the pathological populations. However, in contrast to previous measurements the mean does not evidence any tendency.

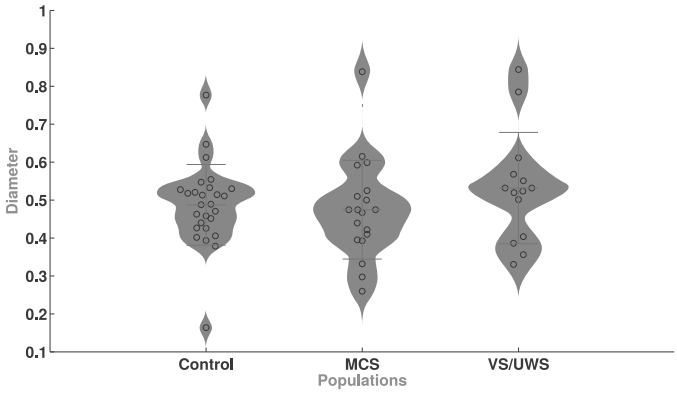

Fig. 4. Distribution of the diameter for healthy control, MCS and VS/UWS patients.

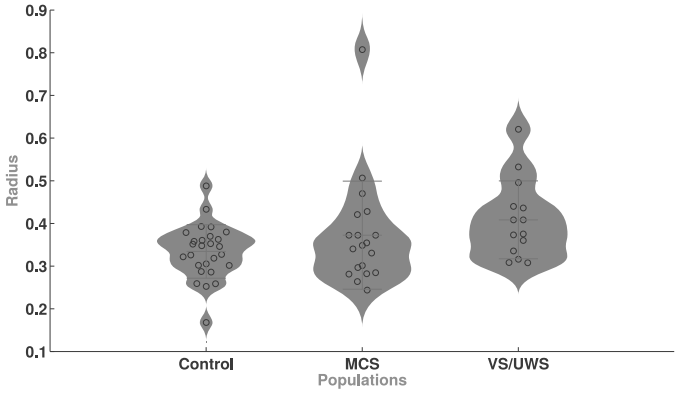

Fig. 5. Distribution of the radius for healthy control, MCS and VS/UWS patients.

The figures 6 and 7 show the results of computing the average strength and average clustering coefficient, respectively. Average strength of healthy control resulted in a major concentration of values around the mean while MCS subjects and VS/UWS evidenced a higher dispersion. The mean values of the strength averages showed a decreasing tendency from healthy controls to MCS and VS/UWS patients.

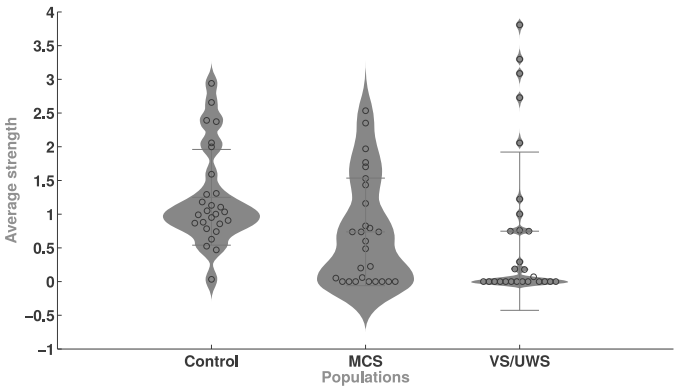

Fig. 6. Distribution of the average strength for healthy control, MCS and VS/UWS patients.

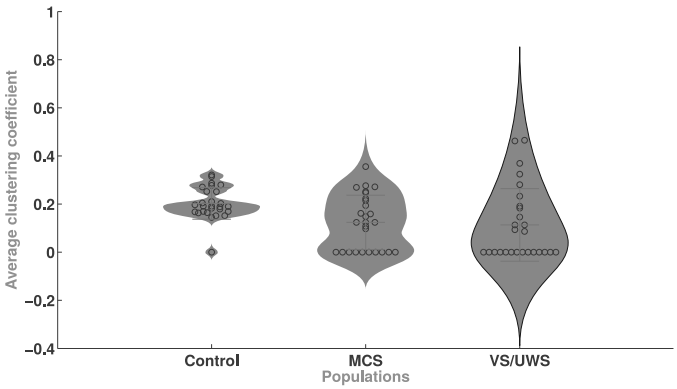

Fig. 7. Distribution of the average clustering coefficient for healthy control, MCS and VS/UWS patients.

Figure 8 shows the mean and standard deviation of each measurement for each population. A comparison between different population groups was performed, as explained in section II-D. As observed five measurements showed statistical differences between healthy controls and DOC patients. Significant differences were also observed between healthy controls and MCS patients for global efficiency, average strength and average clustering coefficient. The comparison between healthy controls and VS/UWS showed also differences for the average characteristic path, diameter and average clustering coefficient. No statistical differences were found for any global measurement between MCS and VS/UWS.

IV. Conclusions

In this paper we study the use of global network measurements to characterize the properties variations of patients with disorder of consciousness (MCS and VS/UWS). Global efficiency, average characteristic path length, average strength and average clustering coefficient have shown that they are sensitive to disorders of consciousness alterations.

Our results suggest that the information efficiency transfer at the global level decrease with the level the severity of the loss of consciousness condition. These results highlight the

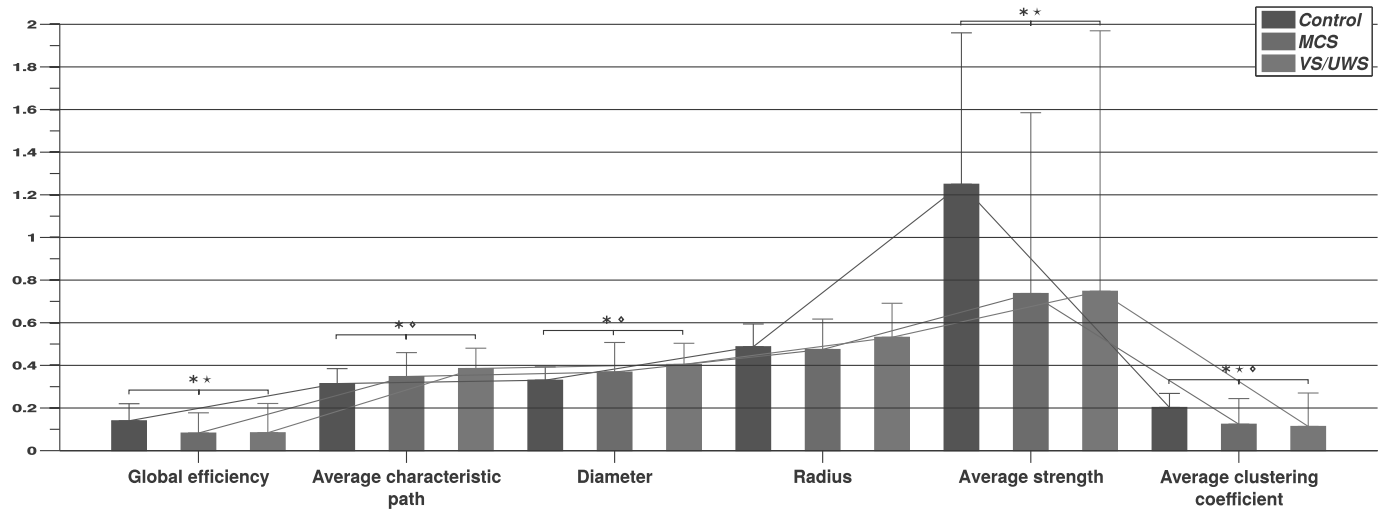

Fig. 8. Global network measurements. Mean and standard deviation of each measurement by population. $*$ $p< 0.05$ in the design one: healthy controls vs. DOC. $\star$ $p< 0.05$ in the design two: healthy controls vs. MCS. $\diamond$ $p< 0.05$ in the design three: healthy controls vs. VS/UWS. $\flat$ $p< 0.05$ in the design four: MCS vs. VS/UWS

importance of graph based features to characterize brain complexity, and in particular, complex phenomena as consciousness emergence. In addition, our results can be potentially used in the development of novel methods to support diagnosis of patients with DOC conditions.

ACKNOWLEDGMENT

This work was supported by the Big Data macro-project from the Cluster in Convergent Technologies from U. Central, the Belgian National Funds for Scientific Research (FNRS), tinnitus Prize 2011 (FNRS 9.4501.12), the European Commission, the James McDonnell Foundation, the European Space Agency, Mind Science Foundation, the French Speaking Community Concerted Research Action, the Belgian interuniversity attraction pole, the Public Utility Foundation "Université Européenne du Travail", "Fondazione Europea di Ricerca Biomedica" and the University Hospital of Liége.

REFERENCES

[1] C. Schnakers and S. Laureys, *Coma and Disorders of Consciousness*. London: Springer, 2012.

[2] S. Laureys and N. Schiff, "Coma and consciousness: Paradigms (re)framed by neuroimaging," *NeuroImage*, vol. 61, no. 2, pp. 478–491, 2012.

[3] J. H. Adams, D. I. Graham, and B. Jennett, "The neuropathology of the vegetative state after an acute brain insult," *Brain*, vol. 123, no. 7, pp. 1327–1338, 2000.

[4] D. Graham, J. Adams, L. Murray, and B. Jennett, "Neuropathology of the vegetative state after head injury," *Neuropsychological Rehabilitation*, vol. 15, no. 3-4, pp. 198–213, 2005.

[5] J. Giacino, J. Fins, S. Laureys, and N. Schiff, "Disorders of consciousness after acquired brain injury: The state of the science," *Nature Reviews Neurology*, vol. 10, no. 2, pp. 99–114, 2014.

[6] J. T. Giacino, K. Kalmar, and J. Whyte, "The {JFK} coma recovery scale-revised: Measurement characteristics and diagnostic utility1," *Archives of Physical Medicine and Rehabilitation*, vol. 85, no. 12, pp. 2020 – 2029, 2004.

[7] C. Schnakers, C. Chatelle, S. Majerus, O. Gosseries, M. De Val, and S. Laureys, "Assessment and detection of pain in noncommunicative severely brain-injured patients," *Expert Review of Neurotherapeutics*, vol. 10, no. 11, pp. 1725–1731, 2010.

[8] J. Whyte, "Rancho los amigos scale," in *Encyclopedia of Clinical Neuropsychology*, J. Kreutzer, J. DeLuca, and B. Caplan, Eds. Springer New York, 2011, pp. 2110–2110.

[9] C. Schnakers, A. Vanhaudenhuyse, J. Giacino, M. Ventura, M. Boly, S. Majerus, G. Moonen, and S. Laureys, "Diagnostic accuracy of the vegetative and minimally conscious state: Clinical consensus versus standardized neurobehavioral assessment," *BMC Neurology*, vol. 9, p. 35, 2009.

[10] D. Cruse, M. Monti, and A. Owen, "Neuroimaging in disorders of consciousness: Contributions to diagnosis and prognosis," *Future Neurology*, vol. 6, no. 2, pp. 291–299, 2011, cited By 1.

[11] J. Gruzelier, "Eeg-neurofeedback for optimising performance. iii: A review of methodological and theoretical considerations," *Neuroscience and Biobehavioral Reviews*, vol. 44, pp. 159–182, 2014.

[12] E. Bullmore, "The future of functional mri in clinical medicine," *NeuroImage*, vol. 62, no. 2, pp. 1267–1271, 2012, cited By 13.

[13] D. Fernández-Espejo, T. Bekinschtein, M. M. Monti, J. D. Pickard, C. Junque, M. R. Coleman, and A. M. Owen, "Diffusion weighted imaging distinguishes the vegetative state from the minimally conscious state," *NeuroImage*, vol. 54, no. 1, pp. 103 – 112, 2011.

[14] V. Calhoun, T. Adali, G. Pearlson, and J. Pekar, "Group ica of functional mri data: seperability, stationarity, and inference." in *Proceedings of International Conference on ICA and BSS*, 2001.

[15] Q. Yu, E. Erhardt, J. c. Sui, Y. d. Du, H. e. He, D. f. Hjelm, M. f. Cetin, S. Rachakonda, R. Miller, G. h. i. Pearlson, and V. e. g. h. Calhoun, "Assessing dynamic brain graphs of time-varying connectivity in fmri data: Application to healthy controls and patients with schizophrenia," *NeuroImage*, vol. 107, pp. 345–355, 2015.

[16] L. Robinson, L. Atlas, and T. Wager, "Dynamic functional connectivity using state-based dynamic community structure: Method and application to opioid analgesia," *NeuroImage*, vol. 108, pp. 274–291, 2015.

[17] B. B. Biswal, "Resting state fmri: A personal history," *NeuroImage*, vol. 62, no. 2, pp. 938 – 944, 2012.

[18] O. Sporns, "Structure and function of complex brain networks," *Dialogues in Clinical Neuroscience*, vol. 15, no. 3, pp. 247–262, 2013.

[19] A. Demertzi, F. Gmez, J. S. Crone, A. Vanhaudenhuyse, L. Tshibanda, Q. Noirhomme, M. Thonnard, V. Charland-Verville, M. Kirsch, S. Laureys, and A. Soddu, "Multiple fmri system-level baseline connectivity is disrupted in patients with consciousness alterations," *Cortex*, vol. 52, no. 0, pp. 35 – 46, 2014.

[20] M. van den Heuvel and O. Sporns, "An anatomical substrate for integration among functional networks in human cortex," *Journal of Neuroscience*, vol. 33, no. 36, pp. 14 489–14 500, 2013.

[21] M. Fraschini, A. Hillebrand, M. Demuru, L. Didaci, and G. Marcialis,

"An eeg-based biometric system using eigenvector centrality in resting state brain networks," *IEEE Signal Processing Letters*, vol. 22, no. 6, pp. 666–670, 2014.

[22] E. b. Santarnecchi, S. Rossi, and A. Rossi, "The smarter, the stronger: Intelligence level correlates with brain resilience to systematic insults," *Cortex*, vol. 64, 2015.

[23] M. D. Fox and M. E. Raichle, "Spontaneous fluctuations in brain activity observed with functional magnetic resonance imaging," *Nature Review Neuroscience*, vol. 8, pp. 700–711, 2007.

[24] C. Rosazza and L. Minati, "Resting-state brain networks: Literature review and clinical applications," *Neurological Sciences*, vol. 32, pp. 773–785, 2011, cited by 68.

[25] Q. Yu, J. g. h. Sui, K. b. Kiehl, G. d. e. Pearlson, and V. c. d. f. Calhoun, "State-related functional integration and functional segregation brain networks in schizophrenia," *Schizophrenia Research*, vol. 150, no. 2-3, pp. 450–458, 2013.

[26] P.-J. Toussaint, S. Maiz, D. Coynel, J. Doyon, A. Messé, L. de Souza, M. Sarazin, V. Perlbarg, M.-O. Habert, and H. Benali, "Characteristics of the default mode functional connectivity in normal ageing and alzheimer's disease using resting state fmri with a combined approach of entropy-based and graph theoretical measurements," *NeuroImage*, vol. 101, pp. 778–786, 2014.

[27] L. J. Larson-Prior, J. M. Zempel, T. S. Nolan, F. W. Prior, A. Z. Snyder, and M. E. Raichle, "Cortical network functional connectivity in the descent to sleep," *Proceedings of the National Academy of Sciences*, vol. 106, no. 11, pp. 4489–4494, 2009.

[28] K. J. Friston, C. D. Frith, P. F. Liddle, and R. S. J. Frackowiak, "Functional connectivity: The principal-component analysis of large (pet) data sets," *J Cereb Blood Flow Metab*, vol. 13, no. 1, pp. 5–14, 1993.

[29] M. van den Heuvel, R. Mandl, and H. Hulshoff Pol, "Normalized cut group clustering of resting-state fmri data," *PLoS ONE*, vol. 3, no. 4, p. e2001, 04 2008.

[30] A. Demertzi, A. Soddu, and S. Laureys, "Consciousness supporting networks," *Current Opinion in Neurobiology*, vol. 23, no. 2, pp. 239–244, 2013, cited By 29.

[31] L. Heine, A. Soddu, F. Gomez, A. Vanhaudenhuyse, L. Tshibanda, M. Thonnard, V. Charland-Verville, M. Kirsch, S. Laureys, and A. Demertzi, "Resting state networks and consciousness. alterations of multiple resting state network connectivity in physiological, pharmacological and pathological consciousness states." *Frontiers in Psychology*, vol. 3, no. 295, 2012.

[32] M. Brier, J. Thomas, A. Fagan, J. Hassenstab, D. Holtzman, T. Benzinger, J. Morris, and B. Ances, "Functional connectivity and graph theory in preclinical alzheimer's disease," *Neurobiology of Aging*, vol. 35, pp. 757–768, 2014.

[33] Y. Hannawi, M. Lindquist, B. Caffo, H. Sair, and R. Stevens, "Resting brain activity in disorders of consciousness: A systematic review and meta-analysis," *Neurology*, vol. 84, no. 12, pp. 1272–1280, 2015.

[34] M. J. Jafri, G. D. Pearlson, M. Stevens, and V. D. Calhoun, "A method for functional network connectivity among spatially independent resting-state components in schizophrenia." *NeuroImage*, vol. 39, pp. 1666–1681, Feb 2008.

[35] G.-R. Wu, W. Liao, S. Stramaglia, J.-R. Ding, H. Chen, and D. Marinazzo, "A blind deconvolution approach to recover effective connectivity brain networks from resting state fmri data," *Medical Image Analysis*, vol. 17, no. 3, pp. 365 – 374, 2013.

[36] U. Sakoglu, G. Pearlson, K. Kiehl, Y. Wang, A. Michael, and V. Calhoun, "A method for evaluating dynamic functional network connectivity and task-modulation: application to schizophrenia," *MAGMA*, vol. 23, no. 5-6, pp. 351–366, Dec 2010.

[37] X. Xie, Z. Cao, and X. Weng, "Spatiotemporal nonlinearity in resting-state fmri of the human brain," *NeuroImage*, vol. 40, no. 4, pp. 1672 – 1685, 2008.

[38] J. Rudas, J. Guaje, A. Demertzi, L. Heine, L. Tshibanda, A. Soddu, S. Laureys, and F. Gomez, "A method for functional network connectivity using distance correlation," in *Engineering in Medicine and Biology Society (EMBC), 2014 36th Annual International Conference of the IEEE*, Aug 2014, pp. 2793–2796.

[39] M. van den Heuvel and O. Sporns, "Network hubs in the human brain," *Trends in Cognitive Sciences*, vol. 17, no. 12, pp. 683–696, 2013.

[40] O. Sporns, "Graph theory methods for the analysis of neural connectivity patterns," in *Neuroscience Databases*, R. Ktter, Ed. Springer US, 2003, pp. 171–185.

[41] E. b. c. Bullmore and O. Sporns, "The economy of brain network organization," *Nature Reviews Neuroscience*, vol. 13, no. 5, pp. 336–349, 2012, cited By 263.

[42] O. Sporns, "The non-random brain: Efficiency, economy, and complex dynamics," *Frontiers in Computational Neuroscience*, no. FEBRUARY, 2011.

[43] M. Rubinov and O. Sporns, "Complex network measures of brain connectivity: Uses and interpretations," *NeuroImage*, vol. 52, no. 3, pp. 1059 – 1069, 2010.

[44] J. Zhou and W. Seeley, "Network dysfunction in alzheimer's disease and frontotemporal dementia: Implications for psychiatry," *Biological Psychiatry*, vol. 75, pp. 565– 573, 2014.

[45] M. b. c. Rubinov and E. b. d. Bullmore, "Fledgling pathoconnectomics of psychiatric disorders," *Trends in Cognitive Sciences*, vol. 17, no. 12, pp. 641–647, 2013.

[46] V. b. Vuksanović and P. b. Hövel, "Functional connectivity of distant cortical regions: Role of remote synchronization and symmetry in interactions," *NeuroImage*, vol. 97, pp. 1–8, 2014.

[47] C. Schnakers, S. Majerus, J. Giacino, A. Vanhaudenhuyse, M.-A. Bruno, M. Boly, G. Moonen, P. Damas, B. Lambermont, M. Lamy, F. Damas, M. Ventura, and S. Laureys, "A french validation study of the coma recovery scale-revised (crs-r)," *Brain Injury*, vol. 22, no. 10, pp. 786–792, 2008.

[48] K. Friston, "Chapter 2 - statistical parametric mapping," in *Statistical Parametric Mapping*, K. Friston, J. Ashburner, S. Kiebel, T. Nichols, and W. Penny, Eds. London: Academic Press, 2007, pp. 10 – 31.

[49] P. Mazaika, F. Hoeft, G. Glover, and A. Reiss, "Methods and software for fmri analysis of clinical subjects," *NeuroImage*, vol. 47, no. Supplement 1, p. S58, 2009.

[50] M. J. McKeown, S. Makeig, G. G. Brown, T. Jung, S. S. Kindermann, A. J. Bell, and T. J. Sejnowski, "Analysis of fmri data by blind separation into independent spatial components," *Human Brain Mapping*, vol. 6, pp. 160–188, 1998.

[51] G. J. Székely, M. L. Rizzo, and N. K. Bakirov, "Measuring and testing dependence by correlation of distances," *The Annals of Statistics*, vol. 35, no. 6, pp. 2769–2794, 2007.

[52] S. Boccaletti, V. Latora, Y. Moreno, M. Chavez, and D.-U. Hwang, "Complex networks: Structure and dynamics," *Physics Reports*, vol. 424, no. 45, pp. 175 – 308, 2006.

[53] E. Bullmore and O. Sporns, "Complex brain networks: graph theoretical analysis of structural and functional systems," *Nature Reviews Neuroscience*, pp. 186 – 198, 2009.

[54] D. J. Watts and S. H. Strogatz, "Collective dynamics of small-world networks," *Nature*, vol. 393, pp. 440–442, 1998.

[55] V. Latora and M. Marchiori, "Efficient behavior of small-world networks," *Physical Review Letters*, vol. 87, p. 198701, Oct 2001.

[56] B. L. Welch, "The generalisation of student's problems when several different population variances are involved." *Biometrika*, vol. 34, pp. 28–35, 1947.